Letters in Applied NanoBioScience
Open-Access Journal (ISSN: 2284-6808)

Article
Volume 12, Issue 4, 2023, 122
https://doi.org/10.33263/LIANBS124.122

Adsorption of Cowpea Husk Extract and Corrosion Inhibition at Interface between X80 Steel and Acidic Oilfield Descaling Fluid

Ekemini Ituen [1,2,3,*], James Asuquo [1], Lin Yuanhua [2,3], Onyewuchi Akaranta [4]

[1] Emerging Materials and Energy Research Group, Department of Chemistry, University of Uyo, Uyo, Nigeria; ekeminiituen@uniuyo.edu.ng (E.I.);
[2] State Key Laboratory of Oil and Gas Reservoir Geology and Exploitation, Southwest Petroleum University, Chengdu 610500, Sichuan, China; yhlin28@163.com (L.Y.);
[3] School of Materials Science and Engineering, Southwest Petroleum University, Chengdu 610500, Sichuan, China; yhlin28@163.com (L.Y.);
[4] African Center of Excellence in Oilfield Chemicals Research, Institute of Petroleum Studies, University of Port Harcourt, Port Harcourt, Nigeria; Onyewuchi.akaranta@uniport.edu.ng (O.A.);
* Correspondence: ebituen@gmail.com (E.I.);

Scopus Author ID 57126213700
Received: 16.03.2022; Accepted: 29.04.2022; Published: 18.09.2022

Abstract: Cowpea husk is an agro-industrial by-product that can be sustainable and cheaply obtained in large quantities. Ethanol extract of the husks (CWPE) was assessed as a corrosion inhibitor for X80 steel in 1 M HCl at 303 – 333 K under static weight loss and electrochemical conditions, accompanied by functional group (FTIR) and surface morphological (SEM) analyses. The inhibition efficiency of 94.6 % and 85.2 % were obtained at 303 and 333 K. CWPE acts as a mixed type corrosion inhibitor with a major influence on the anodic half-reaction and increases charge transfer resistance while decreasing double-layer capacitance and corrosion current density. Corrosion inhibition is attributed to spontaneous adsorption of CWPE phytocompounds on X80 steel surface best approximated by the Langmuir adsorption model. Adsorption is enabled mainly by O, N, and C=C sites affording surface protection and reduced pitting as observed by SEM. CWPE is a potential alternative corrosion inhibitor for X80 steel in mildly acidic environments.

Keywords: adsorption; corrosion inhibition; surface protection; FTIR; SEM.

1. Introduction

Corrosion is a global domestic and industrial problem that causes the deterioration of structural materials, valuable metals, and alloys. The industry's familiar corrosive environments include water, moist air, acids, bases, and salts. Some media such as drilling mud, descaling solutions, formation water, produced water, wastewater, saline or seawater, and brines often encountered in the oilfield are corrosive [1]. Contact of steel construction materials with these media often results in corrosion and subsequent failure of materials with time. Acidic environments are the most corrosive of these media and can be encountered during cleaning/pickling, acid treatment of well, scale washing, reservoir acidizing, etc. To reduce the rate of acid corrosion, corrosion inhibitors, among others, are often added to the acid to be used for the operation.

Corrosion inhibitors are often added in small quantities. They should not reduce the medium's acidity or react with the acid. Therefore, careful design or selection of corrosion inhibitors is important. Inhibitors have been obtained from various natural and synthetic organic molecules [2-4], natural materials [5-7], and several other materials [8-10]. Due to environmental concerns, low cost, and sustainability, many scientists have recently sourced corrosion inhibitors from various plant parts extracts [11-14]. Many potential plant extracts for use as corrosion inhibitors are used for food. Therefore, plant extracts used for the production of corrosion inhibitors mustn't compete with food, which is already in short supply in some communities. Based on this, we considered sourcing corrosion inhibitors from the agro-industrial by-product.

Cowpea husk extract has previously been reported to be efficient in inhibiting aluminum corrosion in 0.5 M NaOH and 0.5 M H_2SO_4 solutions [15]. From our extensive literature search, the potential and application of Cowpea husk extract as a corrosion inhibitor in hydrochloric acid solution, seawater, formation water, descaling or acid wash solution, pickling fluid, and other acidic environments often encountered in petroleum production [16] has not been documented. In this study, we demonstrate and document the application of cowpea husks extract (CWPE) as a corrosion inhibitor for X80 steel in 1 M HCl for the first time. The selection of cowpea husk is informed by previous reports that it contains many classes of phytocompounds similar in structural features to some established corrosion inhibitors. It can also be sourced from farms free of charge, being that it is often disposed of after removing the seeds. Fig. 1 shows the picture of freshly harvested cowpea and dry cowpea husk from which the seed has been removed. The scientific name of the cowpea species used for this study is *Vigna unguiculata*. The corrosion inhibition studies are conducted by weight loss and electrochemical techniques. Complementary techniques like FTIR are used to determine the functional groups associated with the adsorption of CWPE on steel surfaces, while SEM is used to observe the morphology of the steel surface. X80 steel is selected for this study because of its widespread application in constructing pipeworks and reaction vessels [17].

Figure 1. (i) Freshly harvested cowpea made up of seeds and husk (ii) Dry cowpea husk after separation of seeds.

2. Materials and Methods

2.1. Preparation of steel specimens.

Coupons of X80 steel were purchased from Shengxin Technology Co. Ltd, Xinyang, China. The chemical composition was: (wt. %) C (0.17), Si (0.38), Mn (1.25), P (0.015), S (0.002), Mo (0.20), Nb (0.04), Ti (0.015), Fe (bal). Coupon surfaces were treated by degreasing in absolute ethanol, polishing with different grades of silicon carbide, and cleaning following

ASTM procedures [18]. Some coupons were insulated with epoxy adhesives and 1 cm^2 of the surfaces were exposed to be used for electrochemical tests.

2.2. Test solutions.

All reagents used were of analytical grades. HCl was dissolved to 1 M using doubly distilled water. Freshly harvested cowpeas were dried in air at laboratory temperature for one week. The seeds were separated from the husks, and the dried husks were milled and extracted in ethanol. The extract was concentrated using a rotary evaporator and dried to powder in the oven at 40 ^oC. Different masses of dry extract were prepared in 1 M HCl to obtain concentrations 100 ppm to 1000 ppm. The extract has been reported to contain some phenolic compounds such as gallic acid, vanillic acid, syringinc acid, quercetin, myricetin 3-oglcoside caffeic acid, ferulic acid, coumaric acid, and synaptic acid [19].

2.3. Weight loss experiment.

Weight loss was measured after suspending the coupons (dimensions 1 cm x 1 cm x 0.5 cm) in each test solution for 5 hours. Retrieved coupons were cleaned following ASTM standard procedures and then rinsed in acetone to air dry. Triplicates of measurements were made, and average weight loss values were used to calculate corrosion rate. This was repeated at different temperatures from 303 K to 333 K.

2.4. Electrochemical techniques.

Gamry ZRA REF 1800-18042 electrochemical workstation was used for these experiments. The counter, reference, and working electrodes were platinum, saturated calomel electrode (SCE), and X80 steel specimen. The entire assembly and cell were allowed for 30 mins so that corrosion may occur and stabilize the open circuit potential (OCP) before actual measurements were taken [20]. Triplicate experiments were conducted at room temperature (30 ± 2 ^oC), and frequency range of 100 kHz to 10 mHz for EIS, the voltage range of −0.15 V -to + 0.15 V vs. OCP, and a scan rate of 0.2 mV/s for PDP but average values are reported. Gamry E-Chem software was used to analyze data.

2.5. FTIR studies.

A small amount of sample was prepared with KBr into a thin film, and the spectrum was obtained within the range of 350 – 4000 cm^{-1} using a Lasany LI-5500 FTIR Spectrophotometer. After immersion in the inhibited solution for five hours, the surface film on X80 steel was similarly analyzed after washing it with distilled water.

2.6. SEM studies.

X80 steel coupons used were of dimension 1 cm x 1 cm x 0.5 cm. The coupons were immersed in the blank corrodent and the inhibited solution for 5 hours. They were retrieved and cleaned as earlier described, then scanned by SEM.

3. Results and Discussion

3.1. Electrochemical impedance spectroscopy (EIS).

In Fig. 2(i and ii), Nyquist and Bode modulus and phase angle plots, respectively, constructed using experimental data, are shown, and the corresponding EIS parameters deduced are given in Table 1. It can be observed that all the curves show depressed semicircular shapes. This connotes a similar corrosion mechanism for all the test solutions, whether inhabited or not. However, each semicircle intercepts the x-axis at a different distance from the origin, and the diameter of each semicircle increases as the concentration of CWPE increases. This diameter corresponds to solution and charge transfer resistances. Both solution and charge transfer resistances increase as CWPE concentration increases, demonstrating the inhibitive effect of CWPE due to the adsorption of its phytocompounds on the steel electrode surface.

The resulting electrical circuit was modeled using the simple constant phase element (CPE) equivalent circuit model (Fig. 2(iii). By analyzing experimental results using this model, the values of charge transfer resistance (R_{ct}) and solution resistance (R_s) were obtained. Double-layer capacitance, C_{dl} (obtained by using Eq. 1), decreases as CWPE concentration increases, supporting an increase in local dielectric due to the adsorption of CWPE species on the electrode surface. The inhibition efficiency ($\%I_{EIS}$) of CWPE systems was calculated using Eq. 2. A small concentration of CWPE (100 ppm) affords inhibition efficiency as high as 81.7 % at 30 ^{o}C. As concentration increases to 1000 ppm, higher efficiency of 92.0 % was obtained. Thus, inhibition efficiency increases as CWPE concentration increases, similar to other plant extracts previously reported [6].

$$C_{dl} = (Y_0 \, {R_{ct}}^{n-1})^{\frac{1}{n}} \quad (1)$$

$$\%I_{EIS} = 100 \left(\frac{R_{ctI} - R_{ctB}}{R_{ctI}}\right) \quad (2)$$

given that R_{ctB} and R_{ctI} are charge transfer resistances with and without adding CWPE, respectively, n is a constant of the phase angle and Y_o is the CPE constant.

The value of n can be used to infer information on the degree of surface roughness and deviation of the CPE from pure capacitive, resistive or inductive behavior [10]. Being higher (value of n) in the presence of the inhibitor than in the blank shows that surface roughness decreased with the addition of CWPE compared to the absence of CWPE. Adsorption of CWPE species on the steel surface reduces corrosive attack, which in turn decreases the surface inhomogeneity of the electrode, as depicted by an increase in n values as CWPE concentration increases.

Table 1. Some EIS parameters deduced from the Nyquist plot.

Test solution	R_s (Ω)	R_{ct} (Ω)	n	C_{dl}	$\%I_{EIS}$
Blank	0.6723±0.0082	130±2	0.8214	14.29	-
100 ppm CWPE	0.7208±0.0103	710±3	0.8322	9.23	81.7±0.2
500 ppm CWPE	0.9085±0.0105	1126±5	0.8501	3.82	88.5±0.3
1000 ppm CWPE	1.0211±0.0112	1618±9	0.8772	0.28	92.0±0.5

3.2. Potentiodynamic polarization (PDP).

Some potentiodynamic polarization parameters obtained from analyses of experimental results are shown in Table 2, while potentiodynamic polarization curves plotted are shown in Fig. 2(iv). The highest corrosion current density was measured in the uninhibited acid solution, whereas lower currents were obtained in the inhibited solutions. This indicates that the addition

of CWPE reduces corrosion current due to the adsorption of its Phyto-molecules on the electrode (steel) surface, hence the corrosion inhibition effect. Inhibition efficiency ($\%I_{PDP}$) was calculated from the corrosion current densities using Eq. 3, and the obtained efficiency increased when CWPE concentration was raised, similar to EIS results. From Fig. 2(iv), it can be observed that the addition of CWPE displaces the curves toward more positive corrosion potential (E_{corr}). This should imply that CWPE acts as an anodic type corrosion inhibitor. Also, the anodic branches of the potentiodynamic polarization curves are more distorted compared to the cathodic branches. Likewise, there are larger dislodgment in the values of anodic Tafel constants (β_a) of the inhibited solutions than the cathodic constants (β_c) when compared to the 1 M HCl solution. All these reveal that the anodic half-reaction is more influenced by the addition of CWPE due to the corrosion inhibition effect. However, the greatest extent of displacement in E_{corr} is only ±63 mV which is less than ±85 mV required to categorize an inhibitor as an anodic or cathodic type [21]. Thus, CWPE can therefore be viewed to act as a mixed-type inhibitor with domino anodic impact [22].

$$\%I_{PDP} = 100\left(1 - \frac{I^i_{corr}}{I^b_{corr}}\right) \quad (3)$$

where I^b_{corr} and I^i_{corr} are the measured corrosion current densities without and with the addition of CWPE respectively.

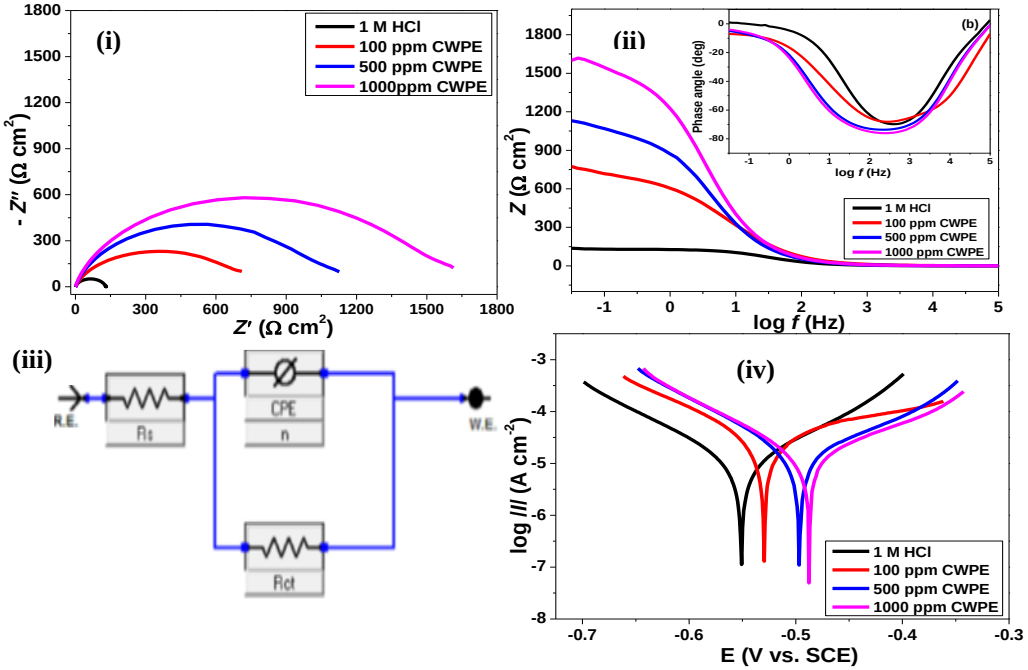

Figure 2. (i) Nyquist plot and (ii) Bode modulus and phase angle plot (iii) Equivalent circuit model and (iv) Potentiodynamic polarization curves for the corrosion of X80 steel in blank 1 M HCl and CWPE inhibited 1 M HCl.

Table 2. Some parameters deduced from PDP curves.

Test solution	I_{corr} (mAcm^{-2})	E_{corr} (V)	β_a ($mVdec.^{-1}$)	β_c ($mVdec.^{-1}$)	$\%I_{PDP}$
Blank	910±5	0.551±0.013	152.8	107.2	-
100 ppm CWPE	156±3	0.529±0.011	138.8	112.1	82.9±0.3
500 ppm CWPE	101±2	0.497±0.008	129.5	110.6	88.9±0.2
1000 ppm CWPE	61±2	0.488±0.010	128.6	109.4	93.3±0.4

3.3 Weight loss.

A weight loss experiment was also conducted to quantify the amount of the X80 steel substrate dissolved due to acid corrosion and corrosion at different temperatures. Weight loss data (Δw) in the presence (w_i) and absence (w_o) of different concentrations of CWPE were used to calculate corrosion rate (CR) according to Eq. 4, while inhibition efficiency ($\%I_{wl}$) was calculated using Eq. 5.

$$CR = \frac{k(w_o - w_i)}{\rho A t} \quad (4)$$

$$\%I_{wl} = 100\left(\frac{CR_0 - CR_1}{CR_0}\right) \quad (5)$$

where k is a factor that converts cmh^{-1} to mmy^{-1} and ρ is the density of iron [23] CR_0 and CR_1 are the corrosion rates without and with the addition of CWPE.

It was observed (Table 3) that without the inhibitor, the corrosion rate was as high as 3.21 mmpy and 14.23 mmpy at 303 K and 333 K, respectively, but reduced to 0.17 mmpy and 2.10 mmpy at 303 K and 333 K respectively on the addition of 1000 ppm CWPE. This corresponds to 94.6 % and 85.2 % inhibition efficiency at 303 K and 333 K, respectively. Inspection of Table 3 also reveals that as temperature increases, the inhibitive effect of CWPE decreases, similar to some plant extracts reported as corrosion inhibitors in literature [24]. CWPE contains various compounds that possess electron-rich potential adsorption sites (see Fig. 3), such as phenolic compounds (e.g., protocatechuic acid, syringic acid) [25], and flavonoids (e.g., quercetin, myricetin 3-Oglcoside) [26] and condensed tannins [27]. Adsorption of these and other phyto-compounds of CWPE on X80 steel surface may have resulted in corrosion inhibition [27].

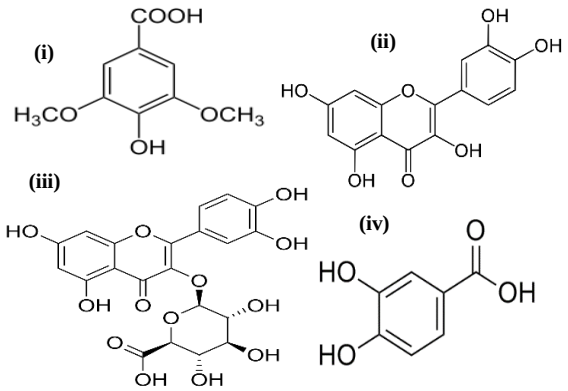

Figure 3. Molecular structures of some compounds in CWPE, namely (i) syringic acid (ii) quercetin (iii) myricetin 3-Oglcoside, and (iv) protocatechuic acid.

Compared to previous reports, CWPE extract was 78 % and 79 % efficient as a corrosion inhibitor for aluminum in 0.5 M NaOH at 303 and 333 K, respectively, and 61 % and 66 % efficient in 0.5 M HCl at 303 and 333 K, respectively [15]. In that report, the efficiency of CWPE increased as temperature increased, which was attributed to the chemical adsorption of CWPE phytochemicals on the aluminum surface. However, our studies with 1 M HCl yield a different trend. Instead, CWPE efficiency decreases when temperature increases, which may be attributed to the physical adsorption of CWPE phytochemicals. Thus, it can be explained that while the aluminum surface favors the chemisorption of CWPE phytocompounds on its surface, adsorption of the same on X80 steel surface is favored by the physisorption mechanism. As found in the present study, CWPE is more efficient for X80 steel surface protection in 1 M HCl at lower temperatures.

Table 3. The corrosion rate of X80 steel in 1 M HCl at different CWPE concentrations and temperatures with the corresponding inhibition efficiency.

Test solution	303 K		313 K		323 K		333 K	
	CR	$\%I_{wl}$	CR	$\%I_{wl}$	CR	$\%I_{wl}$	CR	$\%I_{wl}$
Blank	3.21	-	5.87	-	9.76	-	14.23	-
100 ppm CWPE	0.83	80.4	1.30	77.9	2.52	74.2	4.47	68.6
250 ppm CWPE	0.46	85.7	1.09	81.4	2.21	77.4	3.61	74.6
500 ppm CWPE	0.35	89.2	0.80	86.3	1.79	81.7	3.10	78.2
750 ppm CWPE	0.25	92.1	0.64	89.1	1.50	84.6	2.56	82.0
1000 ppm CWPE	0.17	94.6	0.43	92.6	1.13	88.4	2.10	85.2

3.4. Kinetic and thermodynamic considerations.

The calculated magnitudes of corrosion rate were fixed into the Arrhenius (Eq. 6) and transition state equation (Eq. 7), and line graphs shown in Fig. 4(a-b) were plotted. The apparent activation energy (E_a), enthalpy change (ΔH^*) and entropy change (ΔS^*) of activation (Table 4) were computed from analyses of the plots.

$$\log CR = \log A - \frac{E_a}{2.303RT} \quad (6)$$

$$\log\left(\frac{CR}{T}\right) = \left[\left(\log\left(\frac{R}{Nh}\right) + \left(\frac{\Delta S^*}{2.303R}\right)\right)\right] - \left(\frac{\Delta H^*}{2.303RT}\right) \quad (7)$$

where A is the Arrhenius frequency factor, R is the universal gas constant, T is absolute temperature, N is Avogadro's number, and h is Planck's constant.

It was observed that E_a was lowest in 1 M HCl solution but increased with increasing CWPE concentration. Since E_a is a minimum energy 'wall' for reaction to occur; the addition of CWPE may have increased this barrier, making it difficult for the acid to attack the surface, which implies inhibition of the corrosion [28]. The trend of E_a observed supports physisorption mechanism and agrees with previous literature reports [15,28]. All the ΔH^* values obtained were negative, representing exothermicity while ΔS^* values were a positive signifying association of inhibitor and surface species at the activated complex [29]. Sinc. ΔH^* values are less negative than -40 kJmol^{-1}, the adsorption of CWPE on X80 steel surface was spontaneous and occurred via a physical adsorption mechanism. This implies that the forces that held CWPE species on the steel surface were coloumbic (electrostatic) or weak van der Waals forces. Small and positive values of ΔS^* obtained is consistent with spontaneous exothermic adsorption at the studied temperatures.

Table 4. Activation parameters calculated from Arrhenius and Transition state plots.

CWPE Conc (ppm)	E_a (kJmol^{-1})	A (mmpy)	ΔH^* (kJmol^{-1})	ΔS^* (kJmol^{-1})
0	31.44	1.88 x 10^5	-18.42	0.41
100	34.82	1.96 x 10^6	-32.06	0.33
250	38.03	3.21 x 10^6	-33.71	0.33
500	42.17	4.08 x 10^6	-36.16	0.31
750	44.80	2.01 x 10^7	-38.07	0.30
1000	49.96	3.56 x 10^7	-38.96	0.30

3.5. Adsorption isotherm.

Plant extracts and organic molecules are understood to inhibit corrosion using adsorption. As previously explained, inhibitor molecules first drift from the solution to the surface, where they condense on the surface [30]. Some condensing molecules adsorb and cover a fraction of the surface, while others desorb from the surface depending on the system condition. The fractional surface coverage (θ) was estimated from the obtained inhibition efficiency values (Eq. 8). The values of θ fitted best into the Langmuir adsorption model (R^2

≥ 0.9997) among the several models tested. The Langmuir adsorption isotherm (Fig. 4c) was plotted based on the expression in Eq. 9, and some adsorption parameters were evaluated (Table 5).

$$\theta = E_{wl}/100 \quad (8)$$

$$\frac{C}{\theta} = \frac{1}{K_{ads}} + C \quad (9)$$

where C is the inhibitor concentration, 55.5 represents the concentration of water in the solution, and R is the universal gas constant, K_{ads} represents the inhibitor condensation-evaporation equilibrium constant which can be expressed in terms of the free energy change (ΔG_{ads}) by Eq. 10.

$$\Delta G_{ads} = -RT \ln(55.5K) \quad (10)$$

From Table 4, two things can be observed: first, the values of K_{ads} decreases as temperature increases. This indicates that an increase in temperature shifts the adsorption-desorption equilibrium to the left, favoring the desorption of some previously adsorbed CWPE Phyto-molecules [29]. This also denotes that the inhibitor-steel surface binding power decreases as temperature rises. Secondly, ΔG_{ads} values are all negative and decrease as temperature increases showing that the CWPE molecules adsorbed spontaneously on the steel surface; the spontaneous adsorption becomes less easy as temperature decreases, typical of the physical adsorption mechanism. The values of ΔG_{ads} are less negative than -20 kJmol$^{-1,}$ which fall among the range assigned to the physisorption mechanism [29]. In addition, the slopes were approximately unity in magnitude, which is consistent with the assumptions associated with the derivation of the Langmuir model. This demonstrates that the adsorbed inhibitor species could have formed only a monolayer.

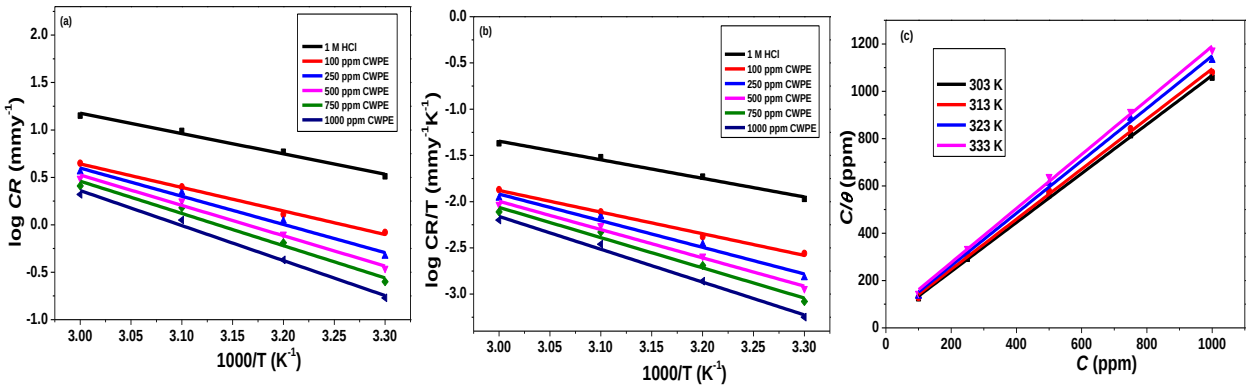

Figure 4. (a) Arrhenius plot and (b) Transition state plot, and (c) Langmuir adsorption isotherm for the inhibition of X80 steel corrosion in 1 M HCl using different concentrations of CWPE at 303 – 333 K.

Table 5. Adsorption parameters calculated from Langmuir adsorption isotherm.

T (K)	Slope	R^2	K_{ads} (x10^3)	ΔG_{ads} (kJmol^{-1})
303	1.03	0.9999	4.01	-15.01
313	1.06	0.9998	3.28	-13.46
323	1.11	0.9998	1.77	-11.85
333	1.13	0.9997	1.24	-11.04

3.6. Corrosion products and mechanistic study.

FTIR studies were conducted to predict the functional groups possibly involved in the adsorption of CWPE on the X80 steel surface. The spectral features of the pure CWPE and the surface adsorbed film scrapped from the X80 steel surface after immersion in the inhibited solution (Fig. 5) were compared. Firstly, it was observed that the spectrum of both substances

was similar, demonstrating that the species on the surface come from the CWPE. Secondly, some of the peaks in the spectrum of the adsorbed film were slightly different in intensity and position than that of the pure CWPE. This indicates that certain functional groups in CWPE were involved in adsorption, which resulted in modifying their vibrational spectral characteristics. As obtained in the present study, changes in FTIR peaks show that the physisorption mode of adsorption was dominant. If chemical adsorption had occurred, there would have been outright disappearance of peaks corresponding to the associated functional groups. Physical adsorption mechanism predicted also collaborates with a prediction made from adsorption studies.

The sharp, intense peaks at1600 -1650 cm^{-1} and 1380 – 1400 cm^{-1} became broad and less intense after adsorption. The 1600 – 1650 cm^{-1} peak may represent C=C, C=O, C=N stretching or N-H bending vibrations, while 1380 – 1400 cm^{-1} could represent O-H bending (phenol, carboxylic, or alcohol). The peaks at 1090 -1100 cm^{-1} (C-O stretching of alcohol, anhydride) and 1150 – 1160 cm^{-1} (C-O stretching of aliphatic ether or tertiary alcohol) can be seen to have resolved to one broad peak after adsorption, similar to the peaks at 1780 (C=O stretching vinyl or phenyl ester) and 1740 cm^{-1}(C=O stretching aldehyde). The medium peak at 3200 – 3500 cm^{-1} corresponding to O-H stretching of alcohol or carboxylic became very broad after adsorption. These show that the adsorption of CWPE could have been facilitated by the listed groups.

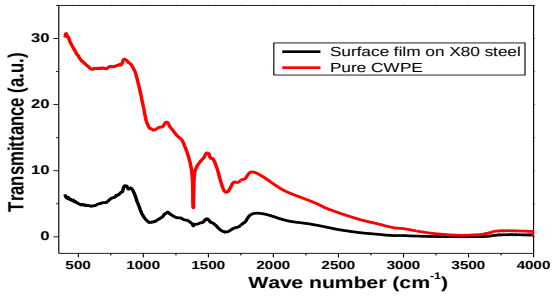

Figure 5. FTIR spectra of pure CWPE (black) and surface adsorbed film on X80 steel.

3.7. Surface examination.

To observe the extent of surface deterioration, the surfaces of the steel in 1 M HCl and CWPE were scanned by SEM. Results (Fig. 6) illustrate that the surface of X80 steel retrieved from the acid solution was harshly damaged, very irregular, and undulant compared to the surface retrieved from the CWPE solution. This supports that CWPE offers protection to the surface and retards the corrosion rate of 1 M HCl. Similar results have been reported by other researchers [30,31].

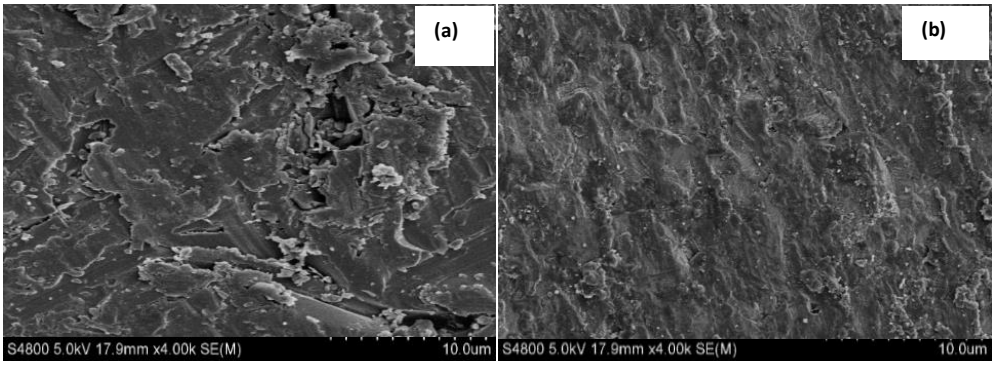

Figure 6. SEM micrographs of X80 steel surface immersed in (a) 1 M HCl and (b) 1 M HCl containing 1000 ppm CWPE.

4. Conclusions

Cowpea husk extract (CWPE) was investigated as a green corrosion inhibitor for steel in a simulated oilfield scale cleaning solution. CWPE is at least 93% and 85% efficient in inhibiting X80 steel corrosion in 1 M HCl at 303 K and 333 K, respectively. The inhibitive effect of CWPE increases as its concentration increases but decreases with a temperature rise. CWPE functions as a mixed-type inhibitor with a predominant effect on the anodic half-reaction. Increased CWPE concentration decreases corrosion current and double layer capacitance but increases charge transfer resistance. CWPE is physically adsorbed on an X80 steel surface enabled by C, N, and O sites from its constituent phyto-compounds. CWPE can be considered a potential eco-friendly anti-corrosion additive for steel surface protection against corrosion in oilfield acid wash solution.

Funding

This research received no external funding.

Acknowledgments

The authors are thankful for the assistance provided by the Natural Science Foundation of China (N0. 52074232).

Conflicts of Interest

The authors declare no conflict of interest.

References

1. Fink, J. *Petroleum engineer's guide to oil field chemicals and fluids.* Gulf Professional Publishing. **2015.**
2. Pradipta, I.; Kong, D.; Tan, J.B. Natural organic antioxidants from green tea inhibit corrosion of steel reinforcing bars embedded in mortar. *Construction and Building Materials* **2019,** *227*, https://doi.org/10.1016/j.conbuildmat.2019.117058.
3. Verma, C.; Hussain, C.M.; Ebenso, E.E. Natural Polymers as Corrosion Inhibitors. In: *Organic Corrosion Inhibitors: Synthesis, Characterization, Mechanism, and Applications*. Eds: Verma, C.; Hussain, C.M.; Ebenso, E.E. **2021**; pp. 411-434, https://doi.org/10.1002/9781119794516.ch18.
4. Hanoon, M.M.; Resen, A.M.; Shaker, L.M.; Kadhum, A.A.; Al-Amiery, A.A. Corrosion investigation of mild steel in aqueous hydrochloric acid environment using N-(Naphthalen-1-yl)-1-(4-Pyridinyl) methanimine complemented with antibacterial studies. *Biointerface Research in Applied Chemistry*. **2021,** *11*, 9735-9743, https://doi.org/10.33263/BRIAC112.97359743.
5. Ituen, E.; Dim, C.; BoEKOM, E. Orange peel extract mediated silver nanofluid as corrosion inhibitor for x80 steel in simulated oilfield scale dissolver. *Journal of Metallic Material Research* **2021**, *4*, 16-25, https://doi.org/10.30564/jmmr.v4i1.3621.
6. Ituen, E.; Akaranta, O.; James, A.; Sun, S. Green and sustainable local biomaterials for oilfield chemicals: Griffonia simplicifolia extract as steel corrosion inhibitor in hydrochloric acid. *Sustainable Materials and Technologies* **2017**, *11*, 12-18, https://doi.org/10.1016/j.susmat.2016.12.001.
7. Salleh, S.Z.; Yusoff, A.H.; Zakaria, S.K.; Taib, M.A.A.; Seman, A.A.; Masri, M.N.; Mohamad, M.; Mamat, S.; Sobri, S.A.; Ali, A.; Ter, T.P. Plant extracts as green corrosion inhibitor for ferrous metal alloys: A review. *Journal of Cleaner Production* **2021**, *304*, https://doi.org/10.1016/j.jclepro.2021.127030.
8. Shang, Z.; Zhu, J. Overview on plant extracts as green corrosion inhibitors in the oil and gas fields. *Journal of Materials Research and Technology* **2021**, *15*, 5078-5094, https://doi.org/10.1016/j.jmrt.2021.10.095.
9. Kumar, A.; Kumar, J. Natural gums as corrosion inhibitor: A review. *Materials Today: Proceedings* **2022**, https://doi.org/10.1016/j.matpr.2022.04.073.
10. Ituen, E.; Singh, A.; Yuanhua, L.; Akaranta, O. Biomass-mediated synthesis of silver nanoparticles composite and application as green corrosion inhibitor in oilfield acidic cleaning fluid. *Cleaner Engineering and Technology* **2021**, *3*, https://doi.org/10.1016/j.clet.2021.100119.

11. Zakaria, F.A.; Hamidon, T.S.; Hussin, M.H. Applicability of winged bean extracts as organic corrosion inhibitors for reinforced steel in 0.5 M HCl electrolyte. *Journal of the Indian Chemical Society* **2022,** *99*, https://doi.org/10.1016/j.jics.2021.100329.
12. Ituen, E.; James, A.; Akaranta, O.; Sun, S. Eco-friendly corrosion inhibitor from Pennisetum purpureum biomass and synergistic intensifiers for mild steel. *Chinese Journal of Chemical Engineering* **2016**, *24*, 1442-1447, https://doi.org/10.1016/j.cjche.2016.04.028.
13. Prasad, D.; Singh, R.; Kaya, S.; el Ibrahimi, B. Natural corrosion inhibitor of renewable eco-waste for SS-410 in sulfuric acid medium: adsorption, electrochemical, and computational studies. *Journal of Molecular Liquids* **2022**, *351*, https://doi.org/10.1016/j.molliq.2022.118671.
14. Ituen, E.; Yuanhua, L.; Verma, C.; Alfantazi, A.; Akaranta, O.; Ebenso, E.E. Multifunctional silver nanocomposite: A potential material for antiscaling, antimicrobial and anticorrosive applications. *JCIS Open.* **2021**, *3*, https://doi.org/10.1016/j.jciso.2021.100012.
15. Abdellattif, M.H.; Alrefaee, S.H.; Dagdag, O.; Verma, C.; Quraishi, M.A. Calotropis procera extract as an environmental friendly corrosion Inhibitor: Computational demonstrations. *Journal of Molecular Liquids* **2021**, *337*, https://doi.org/10.1016/j.molliq.2021.116954.
16. Ituen, E.; Mkpenie, V.; Ekemini, E. Corrosion inhibition of X80 steel in simulated acid wash solution using glutathione and its blends: Experimental and theoretical studies. Colloids and Surfaces A: *Physicochemical and Engineering Aspects* **2019**, *578*, https://doi.org/10.1016/j.colsurfa.2019.123597.
17. Zhang, W.; Li, H.; Chi, Q.; Zhao, X.; Huo, C.; Qi, L.; Li, Y.; Yang, K. Technical specifications for X80 OD 1422 mm line pipes and corresponding products. *Natural Gas Industry B* **2016**, *3*, 485-492, https://doi.org/10.1016/j.ngib.2017.02.009.
18. ASTM G1 Standard Practices for Preparing, Cleaning, and Evaluation of Corrosion Test Specimens Preparation. https://doi.org/10.1520/G0001-03.
19. Mokgope, L.B. *Cowpea seed coats and their extracts: Phenolic composition and use as antioxidants in sunflower oil.* Doctoral dissertation, University of Pretoria. **2007**.
20. Sowmyashree, A.S.; Somya, A.; Kumar, C.P.; Rao, S. Novel nano corrosion inhibitor, integrated zinc titanate nano particles: Synthesis, characterization, thermodynamic and electrochemical studies. *Surfaces and Interfaces* **2021**, *22*, https://doi.org/10.1016/j.surfin.2020.100812.
21. Oubaaqa, M.; Ouakki, M.; Rbaa, M.; Abousalem, A.S.; Maatallah, M.; Benhiba, F.; Jarid, A.; Touhami, M.E.; Zarrouk, A. Insight into the corrosion inhibition of new amino-acids as efficient inhibitors for mild steel in HCl solution: Experimental studies and theoretical calculations. *Journal of Molecular Liquids* **2021**, *334*, https://doi.org/10.1016/j.molliq.2021.116520.
22. Zhang, Q.H.; Li, Y.Y.; Lei, Y.; Wang, X.; Liu, H.F.; Zhang, G.A. Comparison of the synergistic inhibition mechanism of two eco-friendly amino acids combined corrosion inhibitors for carbon steel pipelines in oil and gas production. *Applied Surface Science* **2022**, *583*, https://doi.org/10.1016/j.apsusc.2022.152559.
23. Ahmad, Z. *Principles of Corrosion Engineering and Corrosion Control*. Elsevier, 1st Edition, **2006.**
24. Rosli, N.R.; Yusuf, S.M.; Sauki, A.; Razali, W.M. Musa sapientum (Banana) peels as green corrosion inhibitor for mild steel. In *Key Engineering Materials* **2019**, *797*, 230-239, https://doi.org/10.4028/www.scientific.net/KEM.797.230.
25. Sosulski, F.W.; Dabrowski, K.J. Composition of free and hydrolyzable phenolic acids in the flours and hulls of ten legume species. *Journal of Agricultural and Food Chemistry* **1984**, *32*, 131-133, https://doi.org/10.1021/jf00121a033.
26. Amadioha, A.C.; Nwazuo, E.D. Biochemical Composition of Seed and Husk of Cowpea (Vigna unguiculata (L.) Walp.) Infected by Colletotrichum destructivum O'Gara in Storage. *Annual Research and Review in Biology* **2019**, 1-7, https://doi.org/10.9734/ARRB/2019/v31i130034.
27. Egounlety, M.; Aworh, O.C. Effect of soaking, dehulling, cooking and fermentation with Rhizopus oligosporus on the oligosaccharides, trypsin inhibitor, phytic acid and tannins of soybean (Glycine max Merr.), cowpea (Vigna unguiculata L. Walp) and groundbean (Macrotyloma geocarpa Harms). *Journal of Food Engineering* **2003**, *56*, 249-254, https://doi.org/10.1016/S0260-8774(02)00262-5.
28. Ituen, E.B.; Udo, U.E. Green colloidal composites from local agro-wastes for inhibition of mild steel corrosion in 1M HCl. *Current Journal of Applied Science and Technology* **2018**, *28*, 1-11, https://doi.org/10.9734/CJAST/2018/41824.
29. Ouakki, M.; Galai, M.; Aribou, Z.; Benzekri, Z.; Dahmani, K.; Ech-chihbi, E.; Abousalem, A.; Boukhris, S.; Cherkaoui, M. Detailed experimental and computational explorations of pyran derivatives as corrosion inhibitors for mild steel in 1.0 M HCl: Electrochemical/surface studies, DFT modeling, and MC simulation. *Journal of Molecular Structure* **2022**, *1261*, https://doi.org/10.1016/j.molstruc.2022.132784.
30. Ituen, E.; Akaranta, O.; James, A. Evaluation of performance of corrosion inhibitors using adsorption isotherm models: an overview. *Chemical Science International Journal* **2017**, *18*, 1-34, https://doi.org/10.9734/CSIJ/2017/28976.
31. Abbout, S.; Hsissou, R.; Erramli, H.; Chebabe, D.; Salim, R.; Kaya, S.; Hajjaji, N. Gravimetric, electrochemical and theoretical study, and surface analysis of novel epoxy resin as corrosion inhibitor of carbon steel in 0.5 M H_2SO_4 solution. *Journal of Molecular Structure* **2021**, *1245*, https://doi.org/10.1016/j.molstruc.2021.131014.